

Orbit following calculation of energetic ions for design of ferritic insertion on JT-60U

K. Shinohara, Y. Suzuki, S. Sakurai, K. Masaki, T. Fujita, and Y. Miura
*Naka Fusion Research Establishment, Japan Atomic Energy Agency, Naka, Ibaraki,
 311-0193, Japan*
shinohara.koji@jaea.go.jp

The design work for ferritic inserts is described from the viewpoint of the behavior of energetic ions. The confinement of energetic ions and the absence of the unfavorable heat flux on the first wall was assessed by using the Fully three Dimensional magnetic field OFMC code, which was developed for a ferrite insert program in JFT-2M. In the final design, the confinement of energetic ions is improved by a factor of about 1.3 times in a particular large volume plasma with $B_{t0} = 1.9T$.

1. Introduction

The toroidal field (TF) ripple induces loss of energetic ions due to local mirror trapping (ripple trapped loss) and/or due to lack of the up-down symmetry of banana orbit (banana diffusion). Such enhanced transport of the energetic ions reduces the efficiency of the heating and current drive. To avoid such enhanced transport due to the ripple induced loss, installation of ferritic steel was proposed [1]. The first experiment was carried out on JFT-2M to investigate the reduction of energetic ion loss by using ferritic steel. And the reduction of NB ion loss and the compatibility of ferritic steel with high performance plasmas were demonstrated [2, 3].

Through the valuable experience and results on ferritic insert experiments on JFT-2M, ferritic insertion on JT-60U was proposed. The TF ripple reduction by the ferritic insertion is expected to contribute to the steady-state high-beta plasmas research on JT-60U, because the reduction of energetic ion loss brings: 1) enhancement of the heating and current drive “effective” efficiency, 2) extended pulse length of RF injection due to the reduced heat flux by energetic ions on antennas and, as a result, improved coupling between antennas and a plasma with a smaller gap, 3) availability of wall stabilization without losing the net heating power, and 4) possibility of enhanced availability of the rotation control to improve the MHD stability and transport.

The design work of the ferritic insertion was carried out in 2004, and its installation has finished at the summer of 2005. Here, the design work using orbit following calculations of energetic ions are described. The design work was carried out aiming at effective, machine-safe, and short-term installation. In the design work, the enhanced confinement of energetic ions and absence of the large heat flux on the first wall has been assessed for the NB ions by using the Fully three Dimensional magnetic field Orbit-Following Monte-Carlo code, which was revised from an original code [4] under the ferritic insert program in JFT-

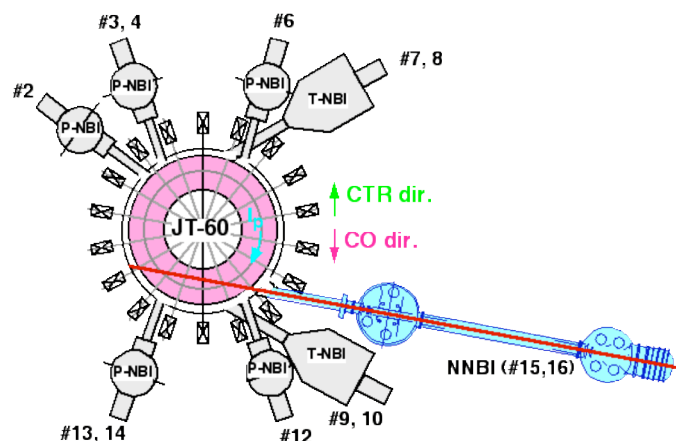


Figure 1. NB systems on JT-60U. #2,3,4,6,12,13,14 are perpendicular PNBS. #7,8,9,10 are tangential PNBS. #15,16 are tangential NNBS. Total power of PNBS is 24.75 MW, and that of NNBS is 4 MW in this calculation.

2M [2].

2. Trials and Final Design

JT-60U has eleven positive ion-based NBs (PNBs) with the injection energy of $\sim 85\text{keV}$ and two negative ion-based NBs (NNBs) with the energy of $350\text{-}420\text{ keV}$. On PNBs, two beams are co-tangential to the direction of the plasma current and the toroidal field, two beams are counter(ctr)-tangential, and seven beams are perpendicular. And NNBs are co-tangential.

As mentioned above, the ripple reduction is expected to bring four benefits mainly. The wall stabilization and better RF efficiency are mainly obtained in a large volume plasma. Thus, our assessment has been carried out intensively for the large volume plasma configuration. An example of the configuration is shown in Fig. 2 (E34797, $t=3.8\text{s}$, $B_t0/I_p =$

$1.86\text{T}/1.1\text{MA}$, $\beta_N = 1.9$, $n_e \sim 1.5 \times 10^{19}\text{m}^{-3}$). At first, the reference results, namely without ferritic steel plates (FP), are shown in Tab 1. The loss of perpendicularly injected beams is large and 63 % of the deposited power. The loss of tangentially injected beams is also not negligible. In the distribution of escaping energetic ions, most of the escaping ions hit on the first wall on the mid-plane of plasma as an orbit loss in this configuration.

We used the ferritic steel with the ingredient of 8Cr-2W-0.2V [5]. This steel has a similar saturation magnetization (1.7T @ 573K) to F82H ferritic steel (8Cr-2W-0.2V-0.04Ta), which is a reduced-activation ferritic steel developed by JAERI [6].

We analyzed several configurations of ferritic insertion in design works. Here, results from three key configurations are shown. In these configurations, we considered only a few important limitations: 1) installation inside vacuum vessel

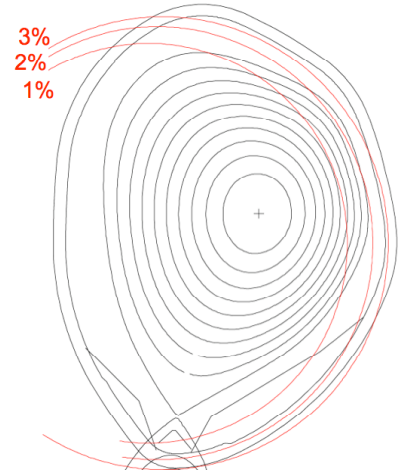


Figure 2. Shape of analyzed large volume plasma with ripple rate contour of TF coils alone.

	Absorbed power for full injection [%]	Loss power for full injection [%]	Absorbed power for perp. PNB [%]	Loss power for perp. PNB [%]	Absorbed power for co. PNB [%]	Absorbed power for ctr. PNB [%]	Absorbed power for co NNB [%]
w/o FP	54	46	40	60	73	59	75
Case I	72	28	63	37	87	67	88
Case II	72	28	63	37	87	69	88
Case III	70	30	61	39	87	68	86
Final Design	68	32	58	42	84	67	84

TABLE 1. POWER FRACTION OF NB ION DESTINATION. FRACTION IS THE RATIO TO THE DEPOSITED POWER IN PLASMA, NOT TO THE INJECTION POWER.

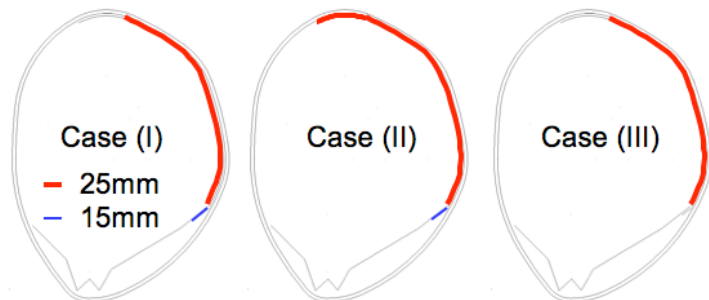


Figure 3 Trial configurations of ferritic insertion, Case (I), (II) and (III). The Note: line thickness is not proportional to the thickness of ferritic steel. The line thickness is exaggerated for illustration.

because a realistic space of its installation is not available outside the vacuum vessel. 2) plate thickness, which should be thinner than that of carbon tiles of 27mm. 3) typical port shape.

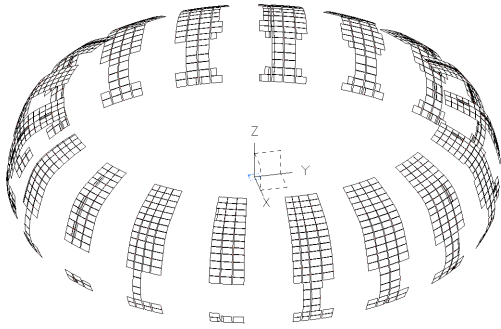


Figure 4. Bird's eye view of ferritic insertion. Thickness of FP is 23 mm

In the case (II), the ferritic inserts are added on the ceiling of the vacuum vessel. Because there is a thin region with relatively large ripple amplitude on the top of the plasma (Fig. 2), which might induce banana diffusion by affecting the excursion of banana tips. The ferritic inserts on the ceiling of the vacuum vessel can reduce the ripple in this region.

In the case (III), the ferritic steel on the baffle board of the divertor was removed compared with the case (I) because the ferrite installation on the baffle board can restrict the operation at high plasma current due to the weak support structure of the baffle board.

The simulation results for these three cases are shown in Tab 1. The differences among these three results are small, but the technical difficulty is increased in the cases of (I) and (II) compared with case (III). From these results, we decided to choose the minimum installation of case (III) as a base of a final design. In the final design, we imposed more restrictions for a realistic installation. The restrictions are: detailed port shapes, e.g. for tangential ports, the interference with diagnostics such as magnetic sensors, the opposed wall of NNB injection. As a result, the 18-fold toroidal symmetry was lost in the magnetic field. The bird's eye view of the ferritic inserts is depicted in Fig. 4. In this configuration, carbon tiles were replaced by ferritic steel on about 10% of the surface area inside the vacuum vessel. The calculation result is shown in Tab 1. Compared with the reference case without FPs, the absorbed power is increased by a factor of about 1.3 times as a whole for a full injection, and the absorbed power of perpendicularly injected beams is increased by a factor of 1.5. We also estimated the heat load on the LH antenna region. The heat load was reduced from 0.6 to 0.2 MW/m² in this particular discharge.

These results are encouraging for our coming experiments. Namely, because of the increases of the absorbed heating power, the MHD stability, the controllability of the current profile, and the controllability of the rotation profile, we are expecting 1) longer discharges with high β_N and high confinement for ITER hybrid scenario, 2) higher β_N beyond an ideal limit of free boundary, 3) longer discharges with high f_{BS} .

3. Dependence on Toroidal Field

Namely, detailed port shape and interference with diagnostics such as magnetic sensors was not taken into account. In these configurations, the ferritic steel was placed in 18 fold toroidal symmetry. The configurations are illustrated in Fig. 3.

The ripple amplitude is large around the mid-plane of the vacuum vessel. In the case (I), the ferritic inserts are placed around the mid-plane as possible in order to reduce the ripple amplitude around the mid-plane. However, because of a relatively weak support structure, the region of ferritic inserts is limited on the baffle board of the divertor.

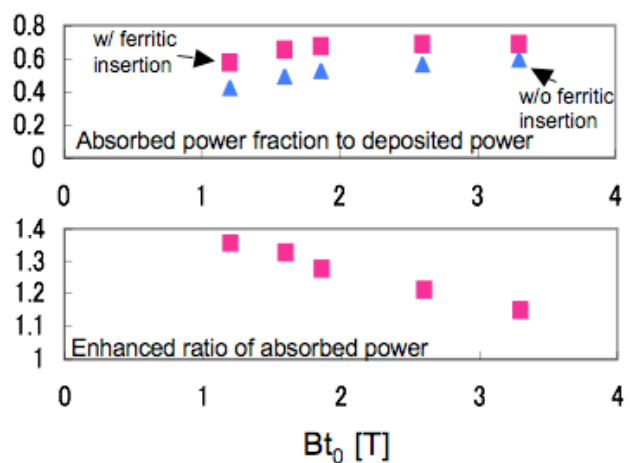


Figure 5. Variation of the absorbed power fraction for cases with and without ferritic insertion, and the ratio of the absorbed power with ferritic insertion to that without ferritic insertion.

Strength

The magnetic field produced by ferritic plates is saturated in above the external vacuum magnetic field of about 0.6 T. Thus, the magnetic field produced by ferritic plates is almost constant in the typical operational toroidal magnetic field, namely $> 1\text{T}$, on JT-60U. This means ferritic plates might “over-cancel” the TF ripple in the lower magnetic field, and work less effectively in the higher magnetic field. It is interesting to investigate the effectiveness of the ferritic

insert in the different strength of the magnetic field produced by TF coils. We have assessed the effectiveness in the magnetic field of 1.2T, 1.6T, 2.6T and 3.3T. The most of the plasma parameter is same with the case of 1.9T. The plasma current and poloidal coil current was varied, depending on the value of the toroidal field. Namely, the safety factor, q , profile is identical to the case of 1.9T.

The strength of the toroidal magnetic field at $R=4.4\text{ m}$ and $Z=0.2\text{m}$ are compared for these 4 cases. The ripple amplitude for 2.6 T and 3.3T is less reduced compared with the case of 1.9 T, however we can see the reduction of the ripple amplitude. In Fig. 5, the

variation of the absorbed power fraction for cases with and without the ferritic insertion and the ratio of the absorbed power with the ferritic insertion to that without the ferritic insertion. The ferritic insertion is less effective for the case of 2.6T and 3.3T, compared with 1.2, 1.6 and 1.9T. Even so, the absorbed power was enhanced by about 1.2 for both the case of 2.6T and 3.3T.

4. Effectiveness of ferritic inserts in a middle-size volume configuration

In the large volume plasmas above analyzed, the major loss is the orbit loss around the mid-plane of the plasmas. Thus it is considered that the final design, in which most of the ferritic plates are installed above the mid-plane, is effective in the large volume plasma, however it was not obvious whether such an installation was effective even in a middle-size volume plasma, in which the ripple trapped loss appears clearly.

We have investigated the effectiveness of ferritic insertion of the final design in a middle-size volume configuration of $B_{t0}/I_p=1.9\text{T}/1.1\text{MA}$. The plasma configuration is shown in Fig. 6. The results of the comparison are shown in Table

2. The ferritic insert of the final design works even in the case of the middle-size configuration. Without ferritic inserts, there are heat loads on the first wall of the downward

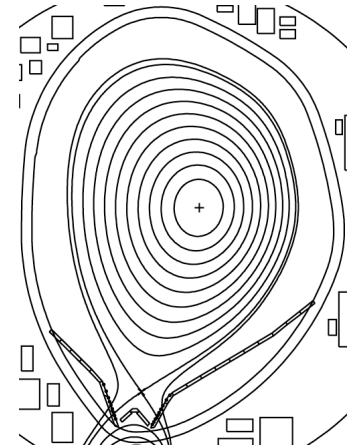


Figure 6. Shape of analyzed middle-size volume plasma

	Absorbed power for full injection [%]	Loss power for full injection [%]	Absorbed power for perp. PNBI [%]	Absorbed power for co. PNBI [%]	Absorbed power for ctr. PNBI [%]	Absorbed power for co NNB [%]
w/o FP	73	27	60	92	76	94
Final Design	81	19	73	95	78	95

TABLE 2. POWER FRACTION OF NB ION DESTINATION. FRACTION IS THE RATIO TO THE DEPOSITED POWER IN PLASMA FOR THE MIDDLE-SIZE VOLUME PLASMA.

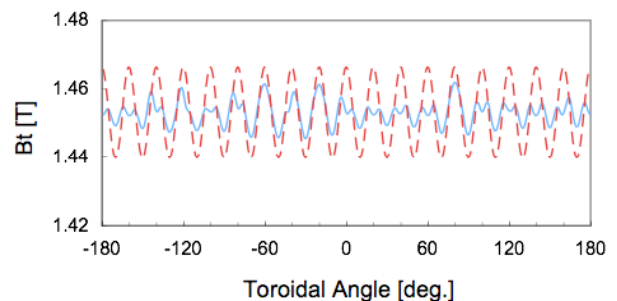


Figure 7. Toroidal variation of the toroidal field strength at $R=4.25\text{m}$ $Z=0.2$

position of plasma. These heat loads come from the ripple trapped loss. With ferritic inserts the heat loads were reduced much. It is considered the ferritic plate around the mid-plane of the vacuum vessel effectively can reduce the TF ripple around the position of the plasma, where it is far from ferritic plates. Fig. 7 shows the toroidal variation of the toroidal field strength at $R=4.25\text{m}$ $Z=0.2$, where is the outer edge on the mid-plane in this configuration. The TF ripple amplitude is reduced even at this position. This result is similar to the experimental results of external ferritic plate installation on JFT-2M [2].

5. Summary

For the further pursuit of the steady-state advanced tokamak research on JT-60U, the ferritic insertion was proposed to reduce the TF ripple. The ripple reduction in large volume plasmas is expected to bring 1) the improved heating and current drive “effective” efficiency, 2) the extended pulse length and the improved efficiency of the RF injection, 3) the availability of wall stabilization without losing heating power, 4) the possibility of the enhanced availability of the rotation control to improve the MHD stability and transport. This proposal of ferritic insertion is based on the successful experience under the ferritic insert program on JFT-2M. In the design work of ferritic insertion, the confinement of energetic ions and absence of the unfavorable heat flux on the first wall was assessed by using the F3D OFMC code, which was developed for a ferrite insert project in JFT-2M.

A large volume plasma of $B_{i0}/I_p=1.9\text{T}/1.1\text{MA}$ was investigated to determine the final configuration of the installation. In the final design, the confinement of energetic ions is improved by a factor of 1.3 for the full injection. We also assessed the effectiveness dependence on the several different toroidal field strengths. Some benefits of ferritic insertion can be available to the higher B_t . A medium sized plasma was also analyzed. The ripple trapped loss was reduced and the confinement of energetic ions is improved by a factor of 1.1.

Acknowledgment

The authors would like to appreciate the JT-60 team and the JFT-2M group for their supports. We would like to acknowledge the support and useful comments of Dr. Y. Kamada of JAEA. We also would like to thank Mr. M. Suzuki of CSK Corporation for his support in the development of the F3D OFMC code.

References

- [1] L. R. Turner, S-T. Wang and H. C. Stevens 1978 Iron shielding to decrease toroidal field ripple in a tokamak reactor Proc. 3rd Topical Meeting on Technology of Controlled Nuclear Fusion (Santa Fe) p 883
- [2] K. Shinohara, et.al. , Nucl. Fusion **43**, 586 (2003)
- [3] K. Tsuzuki, et.al., Nucl. Fusion **43**, 1288 (2003)
- [4] K. Tani, et. al., J. Phys. Soc. Jpn., **50** 1726 (1981)
- [5] Y. Kudo, et al. submitted to J. Korean Phys. Society.
- [6] M. Tamura, et al., J. Nucl. Mater. **155–157** 620–625 (1988).